NEUROSURGICAL FOCUS

Neurosurg Focus 56(4):E7, 2024

Open-door extended endoscopic transorbital technique to the paramedian anterior and middle cranial fossae: technical notes, anatomomorphometric quantitative analysis, and illustrative case

Sergio Corvino, MD,[1–3] Amin Kassam, MD,[4] Amedeo Piazza, MD,[3,5] Francesco Corrivetti, MD, PhD,[3,6] Toma Spiriev, MD,[7] Antonio Colamaria, MD,[8] Giovanni Cirrottola, MD,[8] Carlo Cavaliere, MD, PhD,[9] Felice Esposito, MD, PhD,[1] Luigi Maria Cavallo, MD, PhD,[1] Giorgio Iaconetta, MD,[10] and Matteo de Notaris, MD, PhD[3,10]

[1]Department of Neuroscience and Reproductive and Odontostomatological Sciences, Division of Neurosurgery, Università degli Studi di Napoli "Federico II," Naples, Italy; [2]Department of Neuroscience and Reproductive and Odontostomatological Sciences, PhD Program in Neuroscience, Università degli Studi di Napoli "Federico II," Naples, Italy; [3]Laboratory of Neuroanatomy, EBRIS Foundation, European Biomedical Research Institute of Salerno, Italy; [4]Department of Neurosciences, Intent Medical Group, Northshore University Neurosciences Institute, Arlington Heights, Illinois; [5]Department of Neurosurgery, "Sapienza" University of Rome, Italy; [6]Department of Neurosurgery, San Luca Hospital, Vallo della Lucania, Salerno, Italy; [7]Department of Neurosurgery, Acibadem City Clinic University Hospital Tokuda, Sofia, Bulgaria; [8]Department of Neurosurgery, "Riuniti" Hospital, Foggia, Italy; [9]IRCCS SYNLAB SDN, Naples, Italy; and [10]Neurosurgical Clinic A.O.U. "San Giovanni di Dio e Ruggi d'Aragona," Salerno, Italy

OBJECTIVE The superior eyelid endoscopic transorbital approach (SETOA) provides a direct and short minimally invasive route to the anterior and middle skull base. Nevertheless, it uses a narrow corridor that limits its angles of attack. The aim of this study was to evaluate the feasibility and potential benefits of an "extended" conservative variant of the "standard" endoscopic transorbital approach—termed "open-door"—to enhance the exposure of lesions affecting the paramedian aspect of the anterior and middle cranial fossae.

METHODS First, the authors described the technical nuances of the open-door extended transorbital approach (ODETA). Next, they documented its morphometric advantages over standard SETOA. Finally, they provided a clinical-anatomical application to demonstrate enhanced exposure and better angles of attack to treat lesions occupying the paramedian anterior and middle cranial fossae. Five adult cadaveric specimens (10 sides) initially underwent standard SETOA and then extended open-door SETOA (ODETA to the paramedian anterior and middle fossae). The adjunct of hinge-orbitotomy, through three surgical steps and straddling the frontozygomatic suture, converted conventional SETOA to its extended open-door variant. CT scans were performed before dissection and uploaded to the neuronavigation system for quantitative analysis. The angles of attack on the axial plane that addressed four key landmarks, namely the tip of the anterior clinoid process (ACP), foramen rotundum (FR), foramen ovale (FO), and trigeminal impression (TI), were calculated for both operative techniques and compared.

RESULTS Hinge-orbitotomy of the extended open-door SETOA resulted in several surgical, functional, and esthetic advantages: it provided wider axial angles of attack for each of the target points, with a gain angle of 26.68° ± 1.31° for addressing the ACP ($p < 0.001$), 29.50° ± 2.46° for addressing the FR ($p < 0.001$), 19.86° ± 1.98° for addressing the FO ($p < 0.001$), and 17.44° ± 2.21° for addressing the lateral aspect of the TI ($p < 0.001$), while hiding the skin scar, avoiding temporalis muscle dissection, preserving flap vascularization, and decreasing the rate of bone infection and degree of orbital content retraction.

CONCLUSIONS The extended open-door technique may be specifically suited for selected patients affected by paramedian anterior and middle fossae lesions, with prevalent anteromedial extension toward the anterior clinoid, the foremost compartment of the cavernous sinus and FR and not completely controlled with the pure endoscopic transorbital approach.

https://thejns.org/doi/abs/10.3171/2024.1.FOCUS23838

KEYWORDS extended endoscopic transorbital approach; skull base; open-door technique; orbitotomy; parasellar region; clinoid meningiomas; anterior clinoid process; Meckel's cave

ABBREVIATIONS ACP = anterior clinoid process; FO = foramen ovale; FR = foramen rotundum; GSW = greater sphenoid wing; IOF = inferior orbital fissure; ODETA = open-door extended transorbital approach; SETOA = superior eyelid endoscopic transorbital approach; SOF = superior orbital fissure; TI = trigeminal impression.

SUBMITTED November 14, 2023. **ACCEPTED** January 30, 2024.
INCLUDE WHEN CITING DOI: 10.3171/2024.1.FOCUS23838.

©AANS 2024, except where prohibited by US copyright law

Unauthenticated | Downloaded 10/08/25 05:04 PM UTC

Over the last 50 years, minimally invasive surgery has become the driving paradigm in several branches of surgery, mainly in the neurosurgical field. Particularly, the advent and continuous refinements of endoscopes have led to the progressive and rapid diffusion of their adoption, first in endoscope-assisted and then in purely endoscopic procedures, mainly for pathologies involving the median skull base, as witnessed in the surgical management of sellar region lesions for which the endoscopic endonasal route has become the gold standard.[1,2]

Surgical freedom represents one of the main drawbacks of endoscopic approaches. To overcome this limit, Kassam et al.[3,4] provided some basic rules that allowed, through different additional bony resections, expansion of the surgical corridor and conversion of the "standard" approaches to the "extended" endoscopic endonasal transsphenoidal approaches and consequently to expansion of the surgical indications of this route to lesions extending over the boundaries of the sellar region.[1]

Concerning the superior eyelid endoscopic transorbital approach (SETOA), similar principles apply. Just as Kassam et al. established methods for enhancing the reach of endoscopic endonasal surgery, SETOA also benefits from strategic expansions in technique. SETOA can access pathologies spreading from the anterior skull base up to the petrous apex,[5–9] in an isolated or combined manner,[10,11] through a direct minimally invasive route and provide peculiar advantages.[12,13] Nevertheless, it uses a narrow single corridor compared with those of the binostril endoscopic endonasal approach and is bounded by the bony tissue of the orbital rims superiorly, inferiorly, and laterally and by the vulnerable orbital content medially, which limit its surgical freedom and angles of attack.

In this setting and in line with the concept of the ideal approach—to provide adequate exposure of the lesion and to facilitate its complete and safe resection through identification and protection of adjacent critical neurovascular structures, to improve the maneuverability of surgical instruments at the entry point and surgical target area, and accordingly to provide better control of lesions involving the paramedian aspect of the anterior and middle skull base through better angles of attack and exposure of adjacent neurovascular structures—we tried to expand, in a minimally invasive fashion, the orbital access of the standard SETOA to the middle fossa by converting it to its open-door extended transorbital approach (ODETA) through the placement of two additional bony cuts in a hinge-orbitotomy. Through an anatomical-morphometric quantitative analysis, we compared the horizontal angles of attack between the two considered approaches. Finally, we added an illustrative clinical case of a patient affected by cavernous sinus meningioma and treated with the above-cited technique.

Methods

Five adult cadaveric specimens (10 sides), embalmed and injected with red latex for the arterial blood vessels, were dissected. All dissections were performed in adherence with regulations governing the use of human cadaveric tissues at our institution. No institutional review board approval was required because this study was performed in de-identified cadaveric specimens.

SETOA, after the initial step under exoscopic visualization, proceeded with endoscopic assistance. The osteofibrous flap, which converted the conventional SETOA into its extended open-door variant, was harvested under exoscopic visualization. Both operative techniques were performed on each side of each specimen; to validate our comparison, the approaches were performed in a sequence from the approach with the least tissue removal (standard SETOA) to the one with the most extensive (ODETA).

As previously reported in the pertinent literature,[13] orbital retraction was set at < 10 mm. The axial angles of attack were then analyzed and compared between the two surgical techniques.

Anatomical Dissections

Standard SETOA

SETOA to the petrous apex was performed as previously reported in the pertinent literature.[14] A skin incision was placed in a superior eyelid crease, and subperiosteal/periorbital dissection continued within the orbit to identify the inferior orbital fissure (IOF) and superior orbital fissure (SOF).[15] At this point, the zygomatic body and intraorbital part of the greater sphenoid wing (GSW) were drilled from the anterior end of the SOF proximally to identify and remove the sagittal crest and to expose the temporal pole dura mater distally. Then, interperiosteal dural dissection via the meningo-orbital band[16] was performed to unlock the lateral wall of the cavernous sinus to the gasserian ganglion. After the middle meningeal artery was cut, the temporal pole was elevated in an extradural fashion, and exposure of the greater superior petrosal nerve and the petrous apex completed the dissection procedure (Fig. 1).

Open-Door Extended SETOA

Harvesting the osteofibrous flap straddling the frontozygomatic suture and involving the superior and lateral orbital rims with a hinge-orbitotomy based on the overlying pericranium was used to convert the standard SETOA into its extended open-door variant in three surgical steps (Fig. 2).

In detail, the first step involved widening of the lateral orbital wall for removal (Fig. 2C and F): drilling of the inner surface of the frontal process of the zygomatic bone and the GSW forming the lateral wall of the orbit was extended laterally from the most anterior end of the SOF to reach the most anterior insertion of the temporalis muscle at MacCarty keyhole[17] (Fig. 2C, superior yellow dotted line); then, drilling was continued vertically and inferiorly to follow the anterior border of the temporalis muscle up to the level of the IOF (Fig. 2C, vertical yellow dotted line); finally, drilling was directed medially to reach the most anterior opening of the IOF (Fig. 2C, inferior yellow dotted line).

At that point the orbital rim, including the zygomatic process of the frontal bone and the frontal process of the zygomatic bone, was completely freed from the GSW.

The second and third surgical steps involved performing two osteotomies. Using a reciprocating saw or a cra-

Unauthenticated | Downloaded 10/08/25 05:04 PM UTC

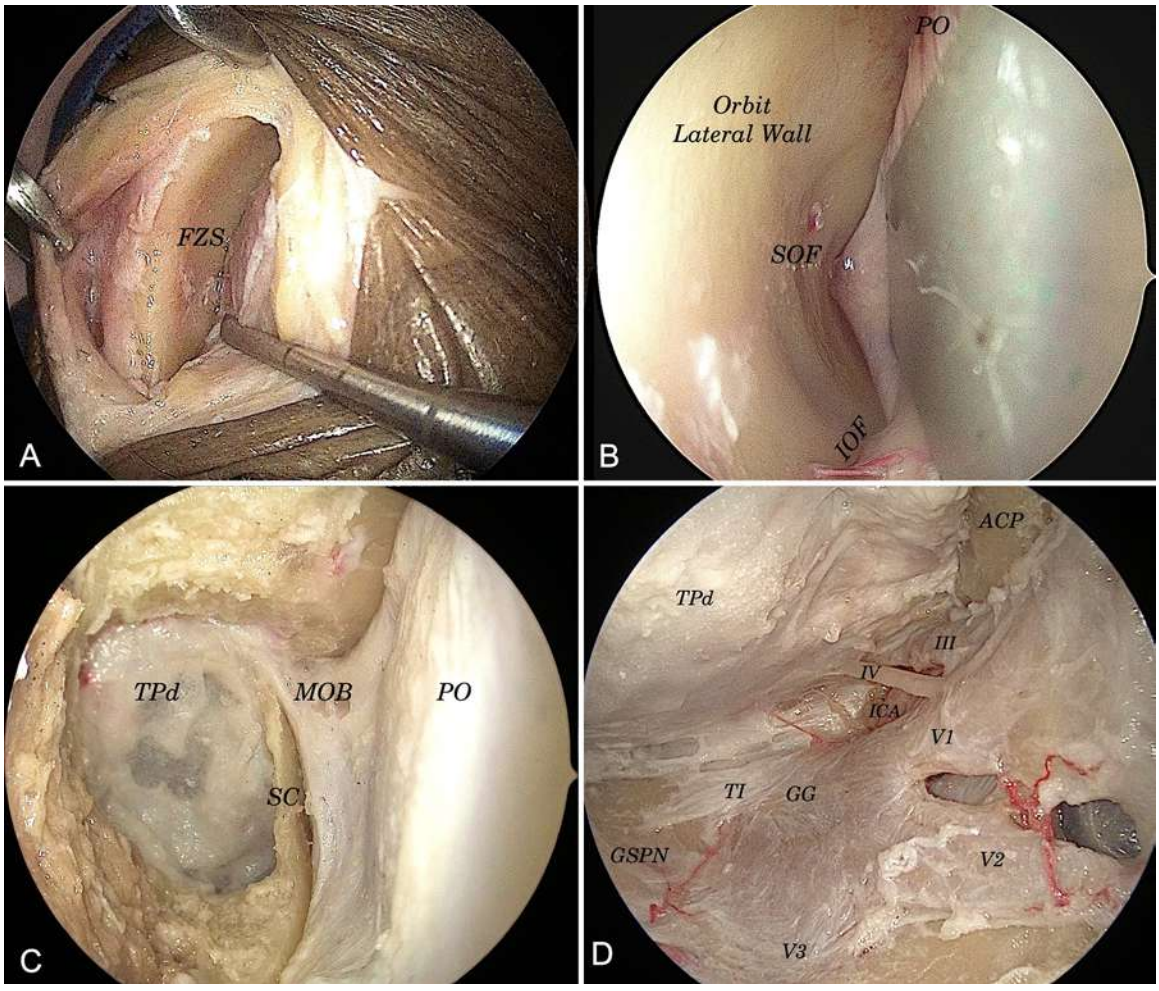

FIG. 1. Common steps during right-sided SETOA and ODETA. **A:** Superior eyelid skin incision and identification of the subperiosteum/periorbital plane of dissection within the orbit and the frontozygomatic suture. **B:** Intraorbital subperiosteal dissection with identification of anatomical landmarks. **C:** Drilling of the lateral orbital wall reveals the temporal pole dura mater, sagittal crest, and meningo-orbital band. **D:** Exposure of the lateral wall of the cavernous sinus after interperiosteal-dural dissection via the meningo-orbital band. FZS = fronto-zygomatic suture; GG = gasserian ganglion; GSPN = greater superficial petrosal nerve; ICA = internal carotid artery; MOB = meningo-orbital band; PO = periorbit; SC = sagittal crest; TPd = temporal pole dura. © Sergio Corvino, published with permission.

niotome without the footplate, we placed two cuts on the exposed superior and lateral orbital rims, straddling the frontozygomatic suture, starting from inside the orbit and preserving the overlying periosteum: the first cut was placed at the level of MacCarty keyhole at the anterior-superior limit of the lateral orbital wall drilling (Fig. 2D, first red dotted line, and Fig. 2G); the second cut was placed at the level of the anterior opening of the IOF at the anterior-inferior limit of the lateral orbital wall drilling (Fig. 2D, second red dotted line, and Fig. 2G). An additional practical technique for these osteotomies involves first accurately locating the frontozygomatic suture. Once this landmark is identified, a superior cut is made 1 cm above it, and a second cut is placed 1 cm below it, ensuring precision in the osteotomies and minimizing the risk of structural compromise or injury to adjacent tissues.

Because the periorbita along the superior and lateral orbital rims is contiguous with the pericranium, the resulting island bone flap is now completely disconnected from the skull bone but is retained in situ in a floating fashion through the overlying pericranium, which acts as a hinge to allow the flap to be dynamically or statically reflected laterally (Fig. 2H).

Anatomical-Morphometric Quantitative Analysis

Axial Angles of Attack

A CT scan was performed on each head specimen before dissections and then uploaded to the Medtronic neuronavigation system. Four target points were identified: the tip of the anterior clinoid process (ACP), foramen rotundum (FR), foramen ovale (FO), and the lateral margin of the trigeminal impression (TI). The angles of attack on the axial plane were measured by fixing the distal tip of the probe on the anatomical target and moving the proximal end of the probe at the orbital content (1 cm retracted), medially, and, at the frontozygomatic suture on

Unauthenticated | Downloaded 10/08/25 05:04 PM UTC

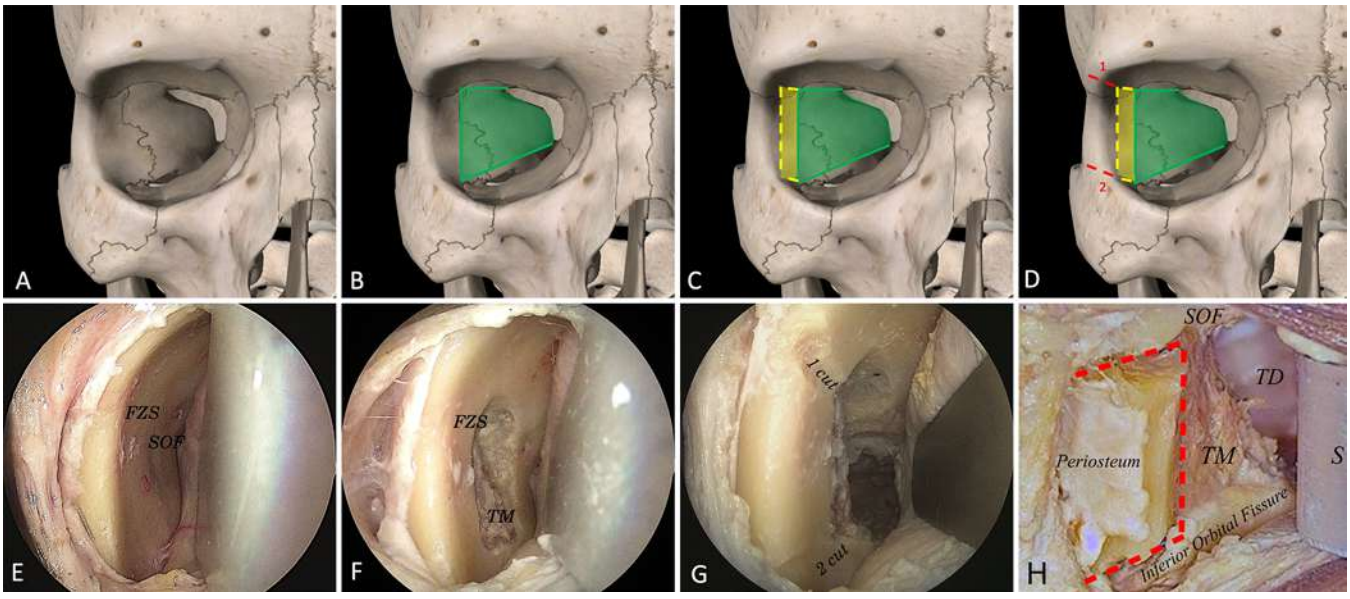

FIG. 2. Steps converting SETOA to ODETA. A–D: Schematic drawings. E–H: Cadaveric dissection (right side). **A:** Bony anatomy of the orbit. **B:** *Green lines* define the boundaries of the lateral orbital wall drilling during standard SETOA. **C:** *Yellow dotted lines* delimit the further lateral orbital wall drilling during the proposed extended open-door SETOA (first step). **D:** Finally, the *two red dotted lines* (*1* and *2*) represent the two bony cuts on the lateral and superior orbital rims, straddling the frontozygomatic suture and realizing the hinge-orbitotomy based on the pericranial flap (second and third steps). **E:** Dissection along the subperiosteum/periorbital plane within the orbit and identification of anatomical landmarks. **F:** Drilling of the lateral orbital wall reveals the inner surface of the temporalis muscle in the homonymous fossa. **G:** Further anterior extension of lateral orbital wall drilling to identify the anterior margin of temporalis muscle and making two shallow grooves identifies the sites of the two bony cuts for the superolateral orbitotomy. **H:** Hinge-orbitotomy based on pericranial flap. The *red dotted line* delimits the area of the osteofibrous flap. FZS = fronto-zygomatic suture; TD = temporal dura; TM = temporalis muscle; S = spatula. © Sergio Corvino, published with permission.

the orbital rim, laterally, for standard SETOA. The lateral boundary of the axial angle for the extended open-door approach was the maximum lateral reflection of the harvested osteofibrous flap without injury of the pericranium and temporalis muscle detachment. These measurements were obtained with the endoscope in position in the surgical field for 12 hours, with a full view of the target, and confirmed on the specimen CT scan that appeared on the neuronavigation system monitor (Fig. 3).

Statistical Analysis

The data of the axial angles of attack related to the ACP tip, FR, FO, and most lateral part of TI, resulting from the standard transorbital approach and from its extended conservative variant, were compared using the Student t-test; $p < 0.05$ was considered statistically significant.

Results

Axial Angles of Attack

The angles of attack in the axial plane for each of the considered targets were wider with ODETA than with the conventional transorbital approach. In detail, the angles described by conventional SETOA were 11.05° ± 1.81°, 10.82° ± 1.65°, 7.14° ± 1.43°, and 6.23° ± 1.32° for addressing the ACP, FR, FO, and TI, respectively, versus 37.73° ± 2.42°, 40.32° ± 2.89°, 27° ± 2.12°, and 23.67° ± 2.23° provided by the extended open-door variant to the same targets, respectively.

The addition of the superolateral hinge-orbitotomy to the conventional endoscopic transorbital approach allowed us to gain 26.68° ± 1.31° in addressing the ACP ($p < 0.001$), 29.50° ± 2.46° in addressing the FR ($p < 0.001$), 19.86° ± 1.98° in addressing the FO ($p < 0.001$), and 17.44° ± 2.21° in addressing the lateral aspect of the TI ($p < 0.001$).

These data are shown in Fig. 3 and summarized in Table 1.

Illustrative Case

A 65-year-old female with a 6-month history of diplopia on the left-sided lateral gaze and hypoesthesia involving the sensory distribution of the maxillary branch of the left trigeminal nerve was observed.

On admission, neurological examination, including comprehensive assessment of ocular motility, visual acuity, and facial sensory changes, revealed moderate deficit of the abducens nerve and mild proptosis in the left eye, while no deficit of visual acuity was detected. Contrast-enhanced MRI of the brain (Fig. 4B and C) showed a lesion with homogeneous contrast enhancement, arising from the dura mater forming the lateral wall of the left cavernous sinus, and a permeative pattern of growth characterized by lateral extension and infiltration of the dura propria of the mesial surface of the ipsilateral temporal pole and consequent compression on the cerebral parenchyma, with medial extension into the cavernous sinus where it displaced medially the internal carotid artery. A head CT

Unauthenticated | Downloaded 10/08/25 05:04 PM UTC

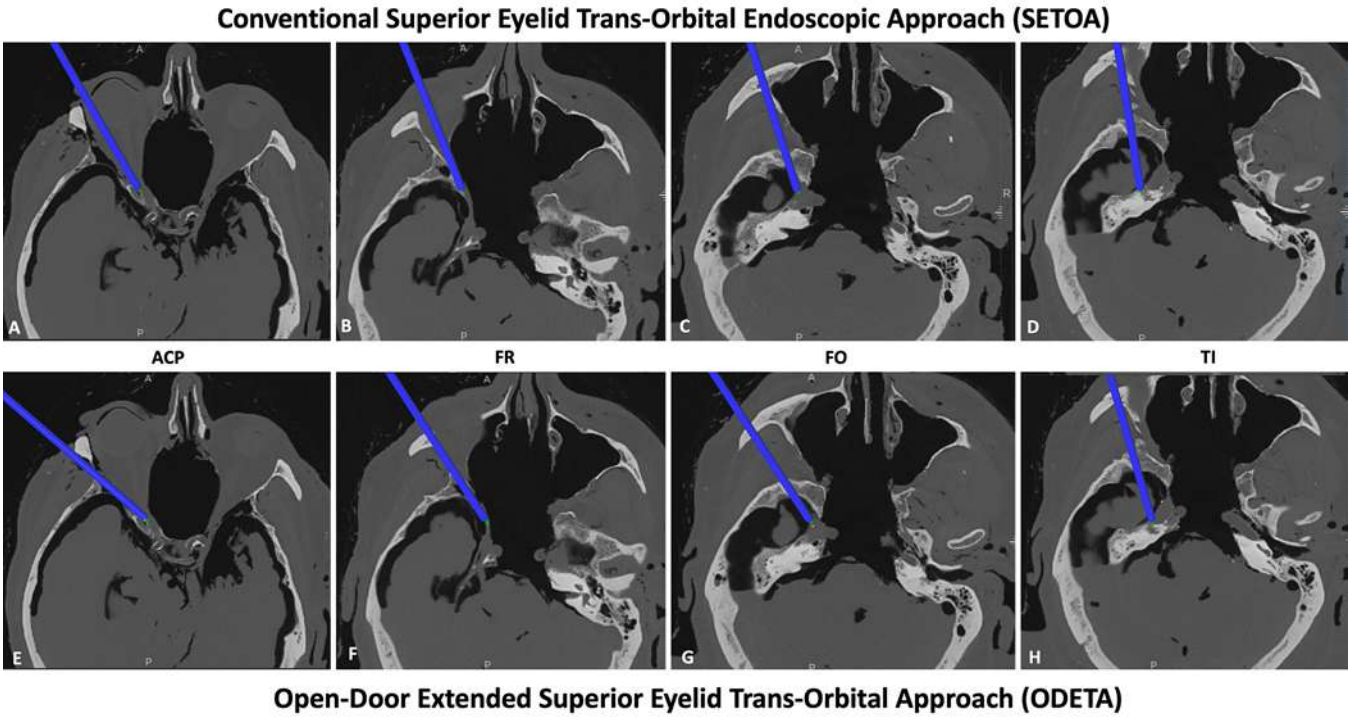

FIG. 3. Neuronavigated CT scans: axial images of horizontal angles of attack (*blue lines*) provided by standard SETOA for addressing the tip of the ACP (**A**), FR (**B**), FO (**C**), and TI (**D**); axial images of horizontal angles of attack (*blue lines*) provided by ODETA for addressing the tip of the ACP (**E**), FR (**F**), FO (**G**), and TI (**H**).

scan (Fig. 4A) detected mild hyperostosis of the intracranial surface of the left GSW and the area around FR. The patient was observed at 6 and 12 months, during which MRI monitoring revealed a slight increase in the volume of the lesion. Because of the radiological progression of the lesion, surgical strategy was offered to the patient, with the aim to prevent/arrest worsening of clinical symptoms.

The patient underwent ODETA to the middle fossa (performed by senior author M.D.N.), as shown in Video 1, with the aim of debulking the extracavernous component of the lesion, through intradural exposure of the dura propria covering the mesial surface of the temporal pole and forming the outer layer of the cavernous sinus lateral wall, and intentionally not entering the neurovascular compartment of the cavernous sinus in order to mitigate the risk of postoperative cranial nerve deficits.

VIDEO 1. Intraoperative video of the open-door SETOA technique to the middle fossa for left cavernous sinus meningioma. © Sergio Corvino, published with permission. Click here to view.

Of paramount importance, the gain angle on axial plain radiography, optimal angle of attack, and slight orbital retraction provided by hinge-orbitotomy allowed for removal of the most anterior and medial extracavernous components of the lesion that were hidden by the posterior content of the orbit. This approach enabled the achievement of the planned goal. The operative time was 2 hours 38 minutes. The postoperative course was uneventful. The diagnosis was in favor of cavernous sinus meningioma WHO grade 1, and the patient received adjuvant radiation treatment for the residual lesion.

Clinical follow-up at 1 month after surgery revealed improvement of diplopia and unchanged V2 hypoesthesia.

TABLE 1. Comparison of the widening of the horizontal angle of attack in standard SETOA and extended open-door SETOA (ODETA)

Anatomical Target	Horizontal Angle of Attack, °		Gain Angle, °	p Value*
	Standard SETOA	ODETA		
ACP	11.05 ± 1.81	37.73 ± 2.42	26.68 ± 1.31	<0.001
FR	10.82 ± 1.65	40.32 ± 2.89	29.50 ± 2.46	<0.001
FO	7.14 ± 1.43	27 ± 2.12	19.86 ± 1.98	<0.001
TI	6.23 ± 1.32	23.67 ± 2.23	17.44 ± 2.21	<0.001

* The Student t-test was adopted; p values < 0.05 were considered statistically significant.

Unauthenticated | Downloaded 10/08/25 05:04 PM UTC

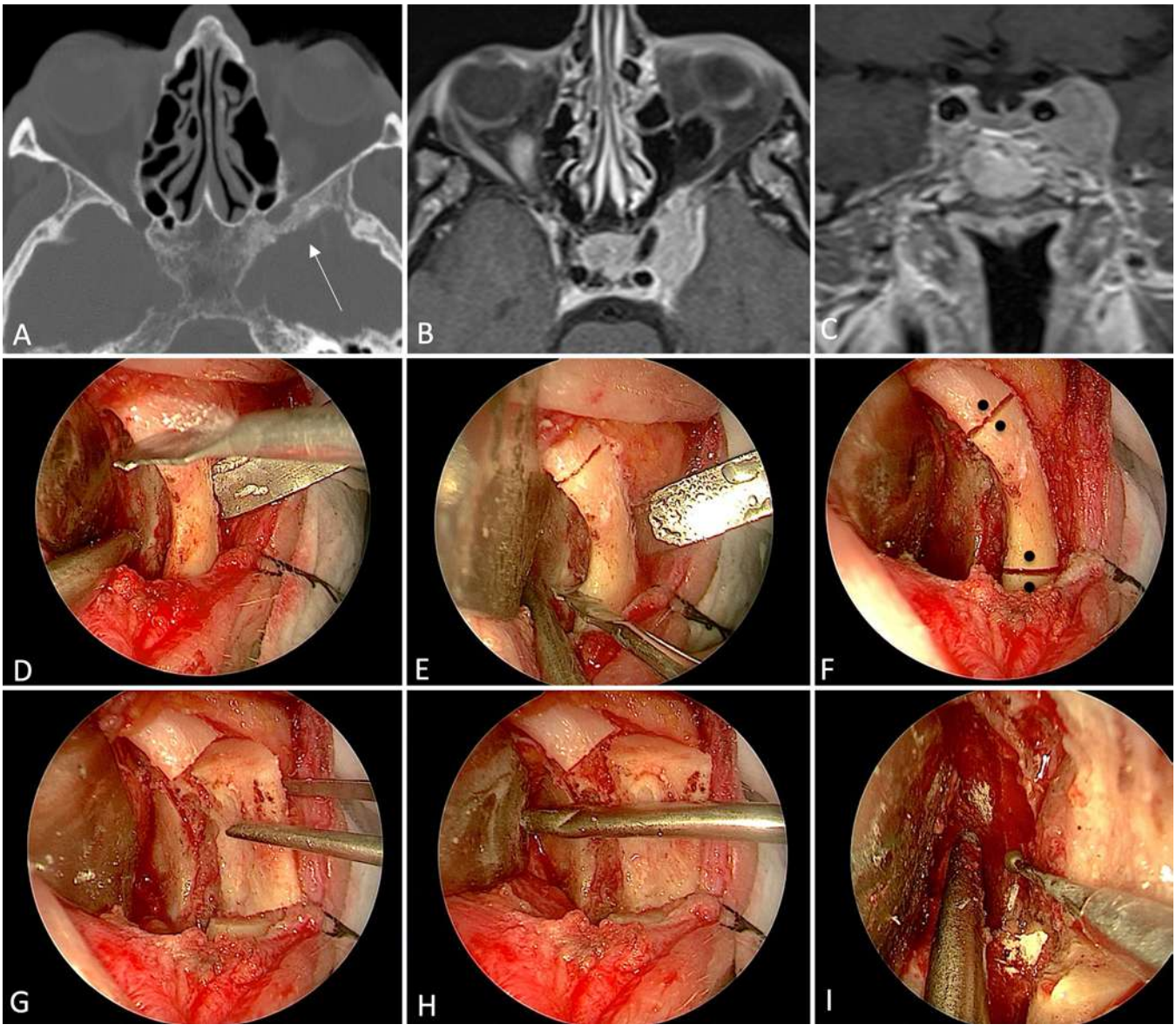

FIG. 4. A: Head CT scan (axial sequence, bone window) is shown. Mild hyperostosis with remodeling of the cancellous bone of the intracranial surface of the left GSW forming the lateral wall of the orbit (*white arrow*), with involvement of the FR. **B and C:** Contrast-enhanced MRI of brain, with T1-weighted axial (B) and coronal (C) sequences. A lesion is shown with homogeneous contrast enhancement arising from the dura forming the lateral wall of the left cavernous sinus, which exhibits a permeative growth pattern, with medial extension to the cavernous sinus, where it displaces medially the internal carotid artery and lateral extension into the intradural space of the medial surface of the temporal lobe. D–I: Intraoperative photographs showing the surgical steps to harvest the osteofibrous flap of the hinge-orbitotomy of ODETA (left side). **D:** The most anterior part of the lateral orbital wall has been drilled; exposure of superolateral orbital rim and positioning of a piezoelectric device in correspondence to the first cut. **E:** The first bony cut is performed and positioning of the piezoelectric device in correspondence to the second cut. **F:** All three steps (drilling of the anterior part of the lateral orbital wall and two bony cuts) to perform hinge-orbitotomy have been performed; the two fixation points used to locate the holes for subsequent suturing of the bone flap are also shown. **G and H:** The osteofibrous flap of the hinge-orbitotomy is laterally displaced. **I:** The surgical procedure is completed with drilling of the deepest part of the lateral wall and sagittal crest removal.

Discussion

Since the introduction of the transorbital neuroendoscopic surgery (TONES) concept by Moe et al.,[13] the neurosurgical indications for the SETOA for intracranial neurosurgical pathologies have rapidly increased.[5] One of the main drawbacks is its narrow surgical corridor defined by the vulnerable orbital content medially and the unexpandable bony tissue of the orbital rims superiorly, laterally, and inferiorly, which limit the angles of attack, particularly for addressing lesions involving the median and paramedian anterior and middle skull base.

To overcome this limit, biportal approaches have been

Unauthenticated | Downloaded 10/08/25 05:04 PM UTC

TABLE 2. Main surgical, functional, and esthetic advantages and limits of open-door extended SETOA (ODETA) compared to standard SETOA and lateral orbitotomy

	ODETA					
	Surgical Procedure		Functional Outcome		Esthetic Outcome	
Approach	Pros	Cons	Pros	Cons	Pros	Cons
vs standard SETOA	Increased horizontal angles of attack	Need for bone reconstruction	Decreased orbital content retraction			
vs lateral orbitotomy		Slightly minor horizontal angles of attack (thickness of bone or orbital rim)	No risk of temporalis muscle atrophy; no risk of facial nerve frontalis branch injury		Scar hidden in a natural eyelid wrinkle; decreased risk of bone flap infection; easier reconstruction	

proposed, both bilateral transorbital and unilateral transorbital combined with transnasal, according to the surgical target area.[10,18–20] Nevertheless, although there is agreement regarding the peculiar advantages resulting from SETOA,[12,13] there is no unanimous consent about the potential benefits provided by the addition of superolateral orbital rim osteotomy.[13,19,21–25]

Noiphithak et al.[21] already addressed this issue, concluding that orbitotomy resulted in a wider exposure area at the entry site and surgical freedom and more favorable horizontal angles of attack, whereas there was no difference in terms of widening of the exposure area of the surgical target and the vertical angles of attack. Contrary to our study, these authors positioned the skin incision on the lateral canthus, dissected the insertion of the temporalis muscle from the superolateral orbital rim and the GSW, limited osteotomy between the frontozygomatic suture and zygoma, and finally removed the bone flap.

More recently, Lim et al.[26] demonstrated significant improvement of horizontal and vertical angles of attack and of surgical freedom, resulting from the addition of superior-lateral orbital rim osteotomy to the transorbital endoscopic approach. Also, this approach of this study considerably differed from our open-door technique, in that the authors placed a different skin incision "below-the-eyebrow" and then created a large free one-piece bone flap that included part of the orbital roof.

In our study, through several key technical nuances, we obtained comparable surgical advantages but with potentially less risk of postoperative comorbidities while creating an enhanced visualization and working corridor. First, by placing the skin incision in a superior eyelid crease, we avoided the potential risk of injury to the frontalis branch of the facial nerve and we hid the scar in a natural wrinkle. Next, by leveraging skin elasticity (which is better in a real patient than a cadaveric specimen), the eyelid incision allowed exposure of the superior orbital rim up to the supraorbital notch and the lateral orbital rim inferiorly to the origin of the root of zygoma, so as to allow us to extend the orbitotomy and accordingly also gain instrumental maneuverability in the vertical plane. In this plane, the orbital area accessed through the open door of the hinge-orbitotomy is from 8 to 10 o' clock according to the "clock model" provided by Paluzzi et al.,[27] which is comparable to the area resulting from lateral micro-orbitotomy.[27] The additional advantages to traditional skull base approaches include 1) preservation of temporalis muscle attachment to the bone, avoiding the risk of atrophy and bleeding; and 2) preservation of the periosteum attached to the orbital rims, in order to preserve vascularization of the flap and theoretically decrease the rate of bone infection and facilitate its attachment to the skull at the end of the procedure.

The blood supply for the outer surface of the upper rim of the orbit and the calvaria is mainly represented by tiny perforators from the overlying periosteum. The vascular interconnections within the periosteum are poorly developed. For this reason, the galea and overlying vascular network should be left broadly attached to the bone when transferring a vascularized calvarial bone flap or a lateral part of the orbit.

We consider all these maneuvers as positive prognostic factors for better functional and esthetic outcomes (Table 2). In terms of the surgical advantages provided, hinge-orbitotomy allowed us to considerably expand the surgical entry site laterally in a dynamic or static way, depending on whether the harvested osteofibrous flap was left free to reflect on the horizontal plane based on the pericranial hinge and according to the instruments' movements or whether it was fixed under a retractor, respectively (Fig. 5). This area is wider in comparison to that resulting from a standard endoscopic transorbital approach, while narrower in comparison to that resulting from lateral orbitotomy with removal of the bone flap just for the osteofibrous flap left in situ. Expansion of the access door resulted in wider angles of attack (Fig. 6). Furthermore, the open-door technique should not be viewed solely as a definitive method to enhance the angle of attack. In cases where it is necessary, the bone can be perfectly dissected from the temporal muscle, converting the technique to a standard lateral orbitotomy. Our recommendation is to approach the lateral orbitotomy in a graded manner, considering the open-door method as the initial step. This adaptability allows for the customization of the surgical approach based on the specific needs presented by the pathology and the individual patient's anatomy.

The more lateral-to-medial trajectories in the axial plane provided by hinge-orbitotomy, along operative corridors almost parallel to the primary anterior-posterior conical vector of the orbit, are mainly favorable for management of lesions affecting the parasellar region including the anterior clinoidal region (i.e., spheno-orbital or clinoidal meningiomas), cavernous sinus (infectious or neoplastic dis-

Unauthenticated | Downloaded 10/08/25 05:04 PM UTC

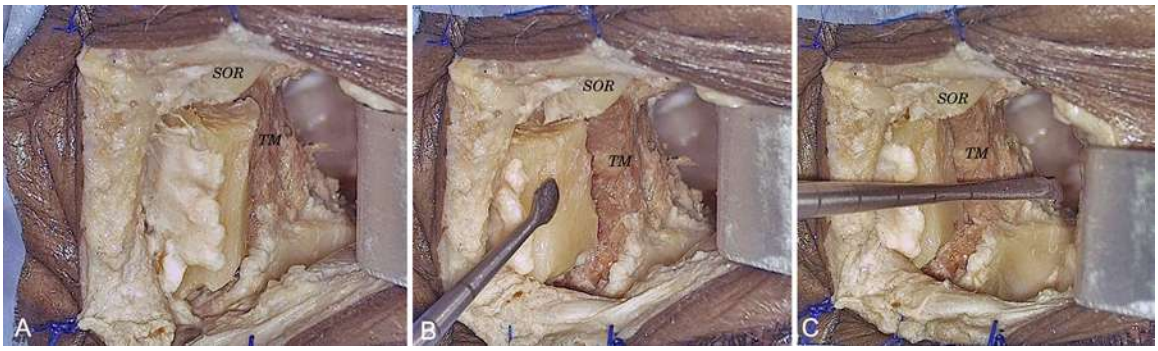

FIG. 5. A: The osteofibrous flap has been harvested in a hinge-orbitotomy. **B:** Lateral displacement of the osteofibrous flap. **C:** Demonstration of the increased lateral-to-medial trajectory of the surgical instrument after dynamic lateral displacement of the harvested osteoplastic flap. SOR = superior orbital rim; TM = temporalis muscle. © Sergio Corvino, published with permission.

eases), Meckel's cave (i.e., trigeminal schwannomas), and petrous apex, in addition to the lateral extraconal ones.[6,26] As witnessed by the results of the present study, the main benefits are obtained in addressing lesions involving the ACP, the most anterior compartment of the cavernous sinus, and/or FR—like for the patient described—where the lateral orbital rim left in situ limits the angle of attack and the orbital content obscures the retro-orbital area.

Last but not least, the extended open-door technique avoided excessive medial retraction of orbital content, thereby decreasing the risk of ophthalmic complications[12,28] related to increased intraocular and/or intraorbital pressure during surgery, which can lead to irreversible vision loss in extreme cases due to hypoperfusion of critical neural structures.[28] This aspect becomes particularly important when treating patients with already high intraorbital pressure, such as those with Grave's orbitopathy or glaucoma, where further increase may be very dangerous.

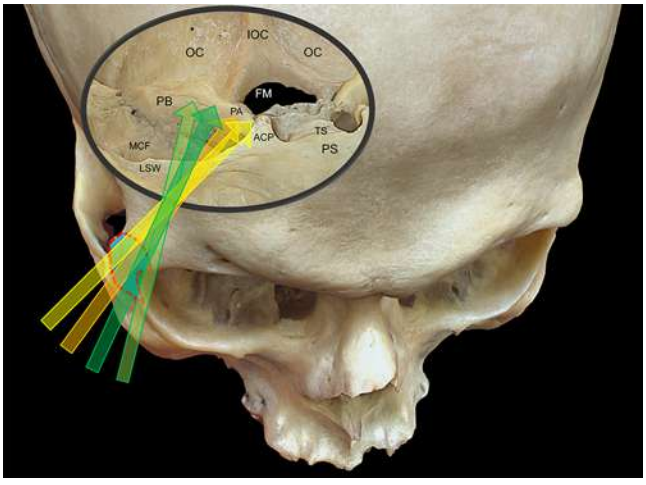

FIG. 6. 3D skull reconstruction. Multiple vectors (*colored arrows*) representing the multiple surgical trajectories gained in the axial plane to address the paramedian anterior and middle skull base after performing hinge-orbitotomy with the extended open-door technique. FM = foramen magnum; IOC = internal occipital crest; LSW = lesser sphenoid wing; MCF = middle cranial fossa; OC = occipital condyle; PA = petrous apex; PB = petrous bone; PS = planum sphenoidale; TS = tuberculum sellae.

In a cadaveric study,[28] an abrupt increase in the intraocular pressure of the orbital content was reported with retraction greater than 1.5 cm; that is why we used 1 cm as the limit for orbital content retraction.

In contrast to the benefits, the main drawback of excessive lateral orbital wall removal and orbitotomy is represented by the risk of enophthalmos.[12] To prevent enophthalmos, reconstruction of the bony defect follows the same principles adopted for conventional SETOA.[12] In addition, when the laterally retracted osteofibrous flap is released, potential venous oozing from the temporalis muscle and the inner table can be identified, as well as from the diploic veins of the flap edges, and meticulous hemostasis can be performed to avoid postoperative hematoma.

The bone flap can be easily secured to the calvaria using low-profile titanium miniplates and screws to achieve anatomical re-approximation of the orbital rim. However, in some cases, patients may be sensitive to the presence of miniplates in such a subtle and delicate skin region. Our technique offers a unique advantage in this regard. Because the bone flap remains attached to the temporalis muscle, it requires only minimal fixation, which can be adeptly achieved using just two nonabsorbable sutures whose fixation points are shown in Fig. 4F. This method contrasts with a standard lateral orbitotomy, where the bone is completely disconnected from the temporalis muscle, necessitating the use of miniplates for secure reattachment in most cases. The suturing method of our approach not only minimizes the palpability and discomfort of the patient but also leverages the inherent stability provided by the temporalis muscle attachment, resulting in a robust reconstruction with enhanced patient comfort.

Finally, we performed the hinge-orbitotomy with exoscopic assistance to increase illumination and visualization of surgical field; nevertheless, because the maneuvers to harvest the osteofibrous flap involve superficial anatomical structures, this technique can also be performed under macroscopic or microscopic visualization.

Superior eyelid endoscopic ODETA represents, in our opinion, a practical compromise between microsurgical orbito-cranial approaches and conventional transorbital endoscopic approaches for selected lesions affecting the paramedian anterior and middle skull base, providing the peculiar benefits resulting from both surgical routes: the

Unauthenticated | Downloaded 10/08/25 05:04 PM UTC

intrinsic advantages of minimally invasive endoscopic surgery—e.g., "eyes of the surgeon close to the surgical field," augmented magnification and illumination, less esthetic disfigurement and bone removal, a short and direct route, avoidance of manipulation of neurovascular structures—and the major surgical freedom and multiple angles of attack allowing for better control of the lesion as with transcranial approaches.

Limitations of This Study

Pure anatomical studies have the common limitation related to cadaveric specimens. The properties of cadaveric tissue, the consistencies of the tissues and their elasticity, and the variability in the trajectories of the cranial nerves differ considerably from those of real-life anatomy.

Conclusions

The hinge-orbitotomy technique provides an expansion of the transorbital corridor with a considerable increase of the axial angles of attack, while reducing orbital content retraction and retaining the bone flap in situ in a "floating" or "hinged" fashion.

This technique preserves the vascularization of the bone flap while decreasing the potential risk of bone infection and improves bone union with the calvaria. The osteoplastic modified SETOA craniotomy is straightforward to perform and enhances exposure of the skull base. Moreover, the vascularized osteofibrous flap can be easily secured to the calvaria, allowing anatomical re-approximation of the orbital rims and offering excellent long-term functional and cosmetic results.

References

1. Miller BA, Ioachimescu AG, Oyesiku NM. Contemporary indications for transsphenoidal pituitary surgery. *World Neurosurg*. 2014;82(6 Suppl):S147-S151.
2. Kasemsiri P, Carrau RL, Ditzel Filho LF, et al. Advantages and limitations of endoscopic endonasal approaches to the skull base. *World Neurosurg*. 2014;82(6 Suppl):S12-S21.
3. Kassam A, Snyderman CH, Mintz A, Gardner P, Carrau RL. Expanded endonasal approach: the rostrocaudal axis. Part I. Crista galli to the sella turcica. *Neurosurg Focus*. 2005; 19(1):E3.
4. Kassam A, Snyderman CH, Mintz A, Gardner P, Carrau RL. Expanded endonasal approach: the rostrocaudal axis. Part II. Posterior clinoids to the foramen magnum. *Neurosurg Focus*. 2005;19(1):E4.
5. Vural A, Carobbio ALC, Ferrari M, et al. Transorbital endoscopic approaches to the skull base: a systematic literature review and anatomical description. *Neurosurg Rev*. 2021; 44(5):2857-2878.
6. Di Somma A, Kong DS, de Notaris M, et al. Endoscopic transorbital surgery levels of difficulty. *J Neurosurg*. 2022; 137(4):1187-1190.
7. Corvino S, Villanueva-Solórzano PL, Offi M, et al. A new perspective on the cavernous sinus as seen through multiple surgical corridors: anatomical study comparing the transorbital, endonasal, and transcranial routes and the relative coterminous spatial regions. *Brain Sci*. 2023;13(8):1215.
8. Corvino S, Armocida D, Offi M, et al. The anterolateral triangle as window on the foramen lacerum from transorbital corridor: anatomical study and technical nuances. *Acta Neurochir (Wien)*. 2023;165(9):2407-2419.
9. de Notaris M, Sacco M, Corrivetti F, et al. The transorbital approach, a game-changer in neurosurgery: a guide to safe and reliable surgery based on anatomical principles. *J Clin Med*. 2023;12(20):6484.
10. Corvino S, Guizzardi G, Sacco M, et al. The feasibility of three port endonasal, transorbital, and sublabial approach to the petroclival region: neurosurgical audit and multiportal anatomic quantitative investigation. *Acta Neurochir (Wien)*. 2023;165(7):1821-1831.
11. Di Somma A, Guizzardi G, Valls Cusiné C, et al. Combined endoscopic endonasal and transorbital approach to skull base tumors: a systematic literature review. *J Neurosurg Sci*. 2022; 66(5):406-412.
12. Corvino S, Sacco M, Somma T, et al. Functional and clinical outcomes after superior eyelid transorbital endoscopic approach for spheno-orbital meningiomas: illustrative case and literature review. *Neurosurg Rev*. 2022;46(1):17.
13. Moe KS, Bergeron CM, Ellenbogen RG. Transorbital neuroendoscopic surgery. *Neurosurgery*. 2010;67(3 Suppl Operative):ons16-ons28.
14. Di Somma A, Andaluz N, Cavallo LM, et al. Endoscopic transorbital route to the petrous apex: a feasibility anatomic study. *Acta Neurochir (Wien)*. 2018;160(4):707-720.
15. Bernardo A, Evins AI, Corvino S. Microsurgical anatomy of the superior and inferior orbital fissures. In: Bonavolontà G, Maiuri F, Mariniello G, eds. *Cranio-Orbital Mass Lesions*. Springer; 2023:17-24.
16. Dallan I, Di Somma A, Prats-Galino A, et al. Endoscopic transorbital route to the cavernous sinus through the meningo-orbital band: a descriptive anatomical study. *J Neurosurg*. 2017;127(3):622-629.
17. Tubbs RS, Loukas M, Shoja MM, Cohen-Gadol AA. Refined and simplified surgical landmarks for the MacCarty keyhole and orbitozygomatic craniotomy. *Neurosurgery*. 2010;66(6 Suppl Operative):230-233.
18. Lim J, Roh TH, Kim W, et al. Biportal endoscopic transorbital approach: a quantitative anatomical study and clinical application. *Acta Neurochir (Wien)*. 2020;162(9):2119-2128.
19. Dallan I, Castelnuovo P, Locatelli D, et al. Multiportal combined transorbital transnasal endoscopic approach for the management of selected skull base lesions: preliminary experience. *World Neurosurg*. 2015;84(1):97-107.
20. Houlihan LM, Loymak T, Abramov I, et al. The biportal transorbital approach: quantitative comparison of the anterior subfrontal craniotomy, bilateral transorbital endoscopic, and microscopic approaches. *J Neurosurg*. 2023;140(1):59-68.
21. Noiphithak R, Yanez-Siller JC, Revuelta Barbero JM, Otto BA, Carrau RL, Prevedello DM. Comparative analysis between lateral orbital rim preservation and osteotomy for transorbital endoscopic approaches to the cavernous sinus: an anatomic study. *Oper Neurosurg (Hagerstown)*. 2019;16(1): 86-93.
22. Chabot JD, Gardner PA, Stefko ST, Zwagerman NT, Fernandez-Miranda JC. Lateral orbitotomy approach for lesions involving the middle fossa: a retrospective review of thirteen patients. *Neurosurgery*. 2017;80(2):309-322.
23. Altay T, Patel BC, Couldwell WT. Lateral orbital wall approach to the cavernous sinus. *J Neurosurg*. 2012;116(4): 755-763.
24. Matsuo S, Komune N, Iihara K, Rhoton AL. Translateral orbital wall approach to the orbit and cavernous sinus: anatomic study. *Oper Neurosurg (Hagerstown)*. 2016;12(4): 360-373.
25. Chen HI, Bohman LE, Emery L, et al. Lateral transorbital endoscopic access to the hippocampus, amygdala, and entorhinal cortex: initial clinical experience. *ORL J Otorhinolaryngol Relat Spec*. 2015;77(6):321-332.
26. Lim J, Sung KS, Kim W, et al. Extended endoscopic transorbital approach with superior-lateral orbital rim oste-

Unauthenticated | Downloaded 10/08/25 05:04 PM UTC

otomy: cadaveric feasibility study and clinical implications (SevEN-007). *J Neurosurg*. 2021;137(1):18-31.
27. Paluzzi A, Gardner PA, Fernandez-Miranda JC, et al. "Round-the-clock" surgical access to the orbit. *J Neurol Surg B Skull Base*. 2015;76(1):12-24.
28. Kim W, Moon JH, Kim EH, Hong CK, Han J, Hong JB. Optimization of orbital retraction during endoscopic transorbital approach via quantitative measurement of the intraocular pressure - [SevEN 006]. *BMC Ophthalmol*. 2021;21(1):76.

Disclosures

The authors report no conflict of interest concerning the materials or methods used in this study or the findings specified in this paper.

Author Contributions

Conception and design: Corvino, Kassam, Piazza, Iaconetta, de Notaris. Acquisition of data: Corrivetti, Corvino, Kassam, Piazza, Colamaria, Cirrottola, Cavaliere, Iaconetta, de Notaris. Analysis and interpretation of data: Corvino, Kassam, Spiriev, Cavaliere, Iaconetta, de Notaris. Drafting the article: Corvino, Kassam, de Notaris. Critically revising the article: Corvino, Kassam, Spiriev, Esposito, de Notaris. Reviewed submitted version of manuscript: Corvino, Kassam, Spiriev, Esposito, Cavallo. Approved the final version of the manuscript on behalf of all authors: Corrivetti. Statistical analysis: Corvino, Kassam, Colamaria, de Notaris. Administrative/technical/material support: Corrivetti, Kassam, Cirrottola, Esposito, Iaconetta. Study supervision: Corvino, Kassam, Colamaria, Esposito.

Supplemental Information

Videos

Video 1. https://vimeo.com/913023864.

Correspondence

Francesco Corrivetti: EBRIS Foundation, European Biomedical Research Institute of Salerno, Italy. corrivettifrancesco@hotmail.it.

Unauthenticated | Downloaded 10/08/25 05:04 PM UTC